

Hemodynamic Changes in Coronary Artery after Stent Implantation Based on Patient-specific Model

Feng Gao and Hiroshi Okada

Department of Mechanical Engineering, Faculty of Engineering and Technology,
Tokyo University of Science, 2641 Yamazaki, Noda, Chiba, 278-8510, Japan
Email: { hokada, gao }@rs.noda.tus.ac.jp

Gang Li

Cardiac Centre of Hebei General Hospital, Shijiazhuang, Hebei 050051, China
Email: hrlg2002@hotmail.com

Abstract—Intravascular stents are tubular structures placed into stenotic artery to expand the inside passage and improve blood flow. The mechanical factors affect the restenosis after stenting and image-based simulation has become a popular tool for acquiring information. The aim of this study was to demonstrate quantitatively and qualitatively the hemodynamic changes in coronary artery after stent implantation based on patient medical image data using computational fluid dynamics (CFD). One patient with coronary artery stenosis before and after stent implantation were included. Based on the CT data, three-dimensional model of pre- and post-stenting models were built. Commercial software Adina8.7 was used for CFD simulation. After stenting, the simulation shows a reduction of wall pressure and wall shear stress and a more equal flow through arteries after stenting. CFD is a noninvasive tool to demonstrate changes of flow rate and flow pattern caused by stent implantation. The effect and possible complications of a stent implantation can be visualized.

Index Terms—Hemodynamics, stent intervention, numerical simulation, coronary artery disease

I. INTRODUCTION

Nowadays stent placement becomes a common interventional procedure for treatment of coronary artery disease and its clinical outcome was better when compared to standard angioplasty [1]. Intravascular stent, which is a small tubular structure, may be driven and expanded inside passage and improve blood flow [2]. However, a process called in-stent restenosis limits the clinical success of coronary stent implantation. It is known that in-stent restenosis is caused by neointimal hyperplasia. The process of neointimal hyperplasia consists of various phases, which includes an inflammatory phase, a granulation or cellular proliferation phase, and a phase of remodeling involving extracellular matrix protein synthesis [3]. The neointimal

hyperplasia is affected by mechanical factors, such as wall strain distribution and blood flow induced wall shear stress [4] and local arterial wall stress [5].

It is difficult to perform the deployment of a stent deployed within a coronary artery and the experimental evaluation is expensive. As a result, computational numerical methods have become as powerful and indispensable method to understand the mechanical behavior of stent implantation. Recently, there has been more and more endeavor to study angioplasty and stenting procedures by means of computational structural analyses [6]-[10]. These studies aim at predicting and calculating the wall stress state generated after a coronary intervention and investigate the role of mechanical factors on the occurrence of restenosis after stenting. Simplified approaches have improved the understanding of the structural properties of coronary stents. However, there is a need to investigate the performance of stent within realistic models of stenosed arteries. There are only a few studies that have utilized patient-specific derived arterial geometries in the structural analysis of stent deployment [11], [12], [13]. The methodology using patient-specific artery model has the potential to provide a scientific basis for optimizing stenting treatment procedures.

Furthermore, coronary arteries are subjected to complex deformation in the cardiac cycle and stents after implantation have permanent plastic deformation at sites where continuous stress occurs, and even have the possibility of inducing fatigue damage, and sometimes fracture [14], [15]. Stent fracture has also been reported in case studies [16], [17], while a broader study showed a stent fracture rate of 24.5% in peripheral arteries at a mean follow up of 10 months [18]. Especially, stenting of bifurcating lesions carries considerably higher risks.

In this work we will demonstrate quantitatively and qualitatively the hemodynamic changes in coronary artery after stent implantation based on patient medical image data using computational fluid dynamics (CFD).

II. METHODES

A. Acquisition of Patient Data

A patient with coronary artery stenosis was involved in this study. The patient was 68 years old male, presented with unstable angina. Coronary angiography revealed luminal obstruction in the middle second of the left anterior descending. The patient was medicated with clopidogrel 300 mg and acetylsalicylic acid 200 mg on the day the angiography was carried out. On the following day, he underwent the implantation of a Cypher Select™ stent (Cordis Corporation, Bridgewater, NJ, USA) and the right femoral artery (RFA) was the access via used. The patient underwent 64-slice CT-scanning both prior to the intervention and after the implantation to obtain CT images data. These data served as an input to generate a 3D geometry models of pre- interventional and post-interventional coronary artery.

B. Geometric Model Reconstruction

The construction process of patient specific model involves the following three major steps: (1) non-invasive image acquisition, (2) imaging process, and (3) three-dimensional reconstruction to form voxel-based volumetric image representation. Original DICOM data (digital imaging and communication in medicine) pre- and post-stenting was transferred to a workstation equipped with Mimics V10.0 (Materialise, Leuven, Belgium) for generation of three dimensional (3D) reconstructed images. Mimics software is a widely-used software in the field of 3D reconstruction. Based on the parameters in the header of images file, Mimics groups the data into sequence. After the raw images of coronary artery were read by Mimics, the operators determined the orientations. Mimics divide the screen into three views: the original axial view of the image, and resliced data making up the coronal and sagittal views. Segmentation of data was performed involving thresholding, region growing, and object creation and separation. The built in gray threshold was used to select coronary to form different mask layers; use "image edit" feature to "add" and "erase" image boundary to increase the precision of the reconstructed image. Also, region growth feature was used to break up the image to obtain more precise coronary voxel. Finally, Mimics 3D calculation feature was used to build up the coronary model (Fig. 1(a)). After segmentation, 3D models were created using the module of 3D calculation from selected mask which is available in the Mimics software package, and the 3D surface were exported in STL (stereo lithography), a common format for computed-aided design.

C. Generation of Mesh Models

STL files for pre- and post-stenting models were imported into ADINA 8.7 (ADINA R & D, Inc., USA). ADINA creates the necessary points, body edges and faces that can be used to define finite element meshes and also loads and boundary conditions. The pre- and post-stenting models were generated by tetrahedral volume meshes using ADINA-F. Fig. 1(b)(c) shows the mesh model for pre- and post-stenting model. The pre- and

post-stenting models were composed of 39,925 and 94,139 elements, respectively.

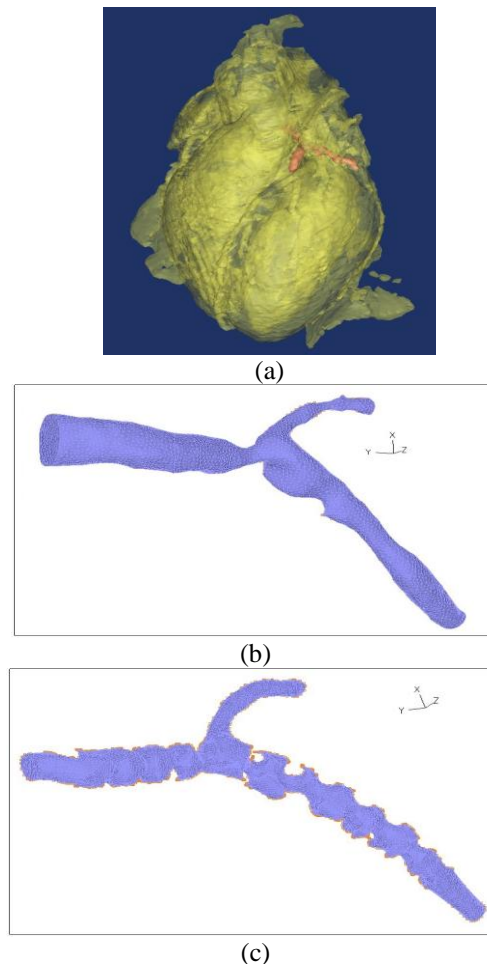


Figure 1. (a) Coronary artery bifurcation is shown in relation to the heart. (b) Mesh model of pre-stenting coronary artery. (c) Mesh model of post-stenting coronary artery.

D. CFD Simulations

Average physiological hemodynamic conditions with steady flow have been considered for the 3D numerical simulations. The blood was assumed to behave as a Newtonian fluid. The viscosity was set to 0.0035 Pa·s and the density to 1060 kg/m³, corresponding to the standard values cited in the literature [19].

Given these assumptions, the fluid dynamics of the system are fully governed by the Navier-Stokes equations, which provide a differential expression of the mass and momentum conservation laws. The reference value 0.2 m/s [20] of the flow velocity was applied at the inlet for both models. The flow was assumed to be incompressible and laminar. A zero traction force outlet boundary condition was applied to both outlets. The ADINA 8.7 is used to numerically simulate the blood flow in pre- and post-stenting coronary models.

III. RESULTS

Hemodynamic analysis was successfully performed in both pre- and post-stenting models. Flow pattern, wall

pressure, and wall shear stress before and after stent implantation were visualized and compared.

A. Flow Pattern

The flow rate in pre- and post-stenting models was measured. The maximum flow rate before stent implantation was 2.938 m/s. After stent implantation, the maximum flow rate decreased to 1.602 m/s.

Fig. 2 and Fig. 3 show the flow pattern in pre- and post-stenting coronary artery model. In the pre-stenting model, the flow pattern showed areas of high velocity in the stenosis near the bifurcation and low velocity in the region of inlet, which is the greatest diameter of coronary artery. There are small eddies visible at the bifurcation behind the stenosis. In the post-stenting model, the velocity is decreased while it is higher inside the stent wire to the smaller diameter. There are eddies appeared between the stent wires.

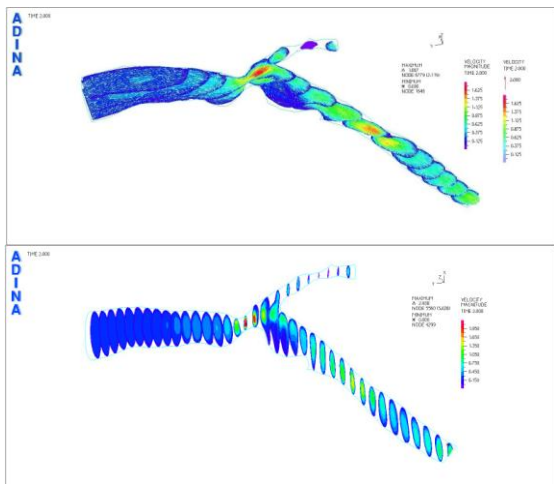


Figure 2. Flow pattern in pre-stenting coronary artery model.

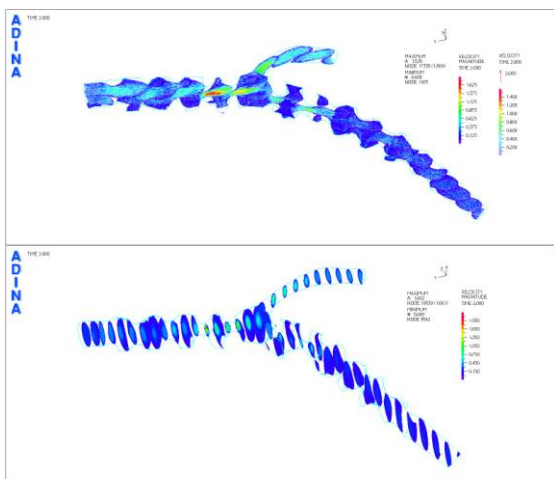


Figure 3. Flow pattern in post-stenting coronary artery model.

B. Pressure

Fig. 4 and Fig. 5 show the pressure distribution in pre- and post-stenting models. In the pre-stenting model, the areas of high pressure were situated before the stenosis. The pressure dropped significantly at the stenosis. At the

area of bifurcation, the pressure is elevated a little. In the post-stenting model, the pressure is much lower compared with pre-stenting model. Inside the stent, it dropped smoothly before the bifurcation.

C. Wall Shear Stress

Fig. 6 and Fig. 7 show the wall shear stress in pre- and post-stenting models. The areas of high wall shear stress are similar to the high velocity. In the pre-stenting model, the area of highest wall shear stress is situated in the stenosis. In the post-stenting model, the areas of high wall shear stress are inside the stent wire. The maximum shear stress is decreased in the pre-stenting model than in the post-stenting model.

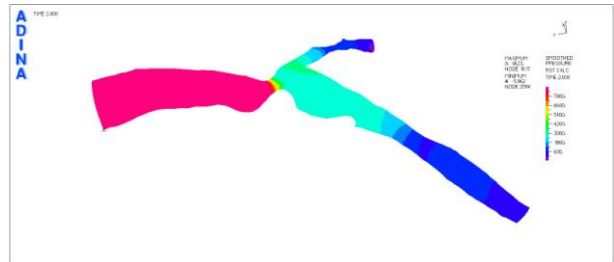


Figure 4. Pressure distribution in pre-stenting coronary artery model.

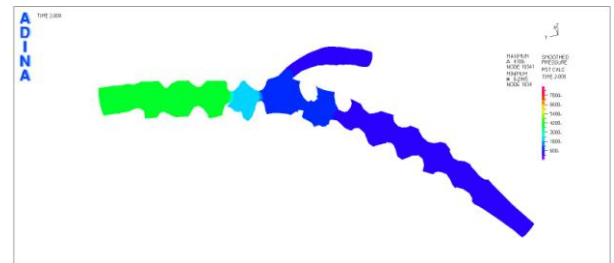


Figure 5. Pressure distribution in post-stenting coronary artery model.

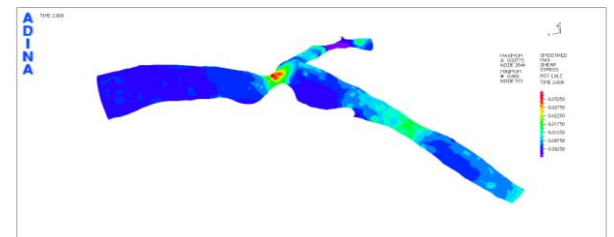


Figure 6. Wall shear stress in pre-stenting coronary artery model.

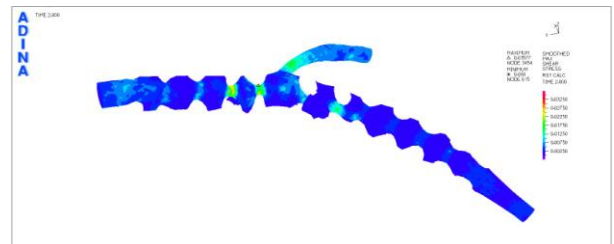


Figure 7. Wall shear stress in post-stenting coronary artery model.

IV. DISCUSSION AND CONCLUSION

Stent implantation is a minimally invasive procedure for treatment of coronary artery stenosis. This study

investigates the hemodynamic changes of stent implantation based on patient specific pre- and post-stenting models.

Construction of patient specific model often starts from the acquisition of anatomic data from an appropriate medical imaging modality. The CT images are integrated using 2D segmentation and 3D region growth. Through three-dimensional anatomic view, meaningful images are extracted from the volumetric image data. These three-dimensional images lead to the generation of anatomic modeling. We obtained the coronary artery CT images from patient both before and after stenting. After the 3D entity reconstruction of the coronary blood, we successfully get the model of pre- and post-stenting coronary.

The quantitative results of CFD simulation in pre- and post-stenting models show a more equal blood flow volume through the coronary artery and a smoother flow pattern. The reason for this is the new geometry after stent implantation. And the reductions of pressure and wall shear stress were found in the post-stenting model. As discussed in more detail by Moore et al. [21] wall shear stress variations are considered significant only if they would lead to different conclusions regarding the links between hemodynamics and coronary artery disease. Recent histological studies show that eccentric intimal thickening occurs predominantly along the inner wall of the coronary artery proximal region and may be attributable to a combination of low wall shear stress. The new geometry produced alternating regions of low wall shear stress on post-stenting model, which could be important in the localization of atherogenesis for restenosis.

We were able to demonstrate quantitative and qualitative hemodynamic changes after stent-graft implantation in patient specific model using CFD simulation. Future analyses will address the effects of fluid structure interaction between blood flow and coronary artery wall for stent implantation.

REFERENCES

- [1] P. W. Serruys, P. de Jaegere, and F. Kiemeneij, "A comparison of balloon-expandable-stent implantation with balloon angioplasty in patients with coronary artery disease," *Benestent Study Group. N Eng J Med*, vol. 331, pp. 489-495, 1994.
- [2] C. T. Dotter, "Transluminally-placed coil spring end arterial tube grafts, long-term patency in canine popliteal artery," *Investigative Radiology*, vol.4, pp. 329-332, 1969.
- [3] E. R. Edelman and C. Rogers, "Pathobiologic responses to stenting," *Am J Cardiol*, vol. 81, pp. 4E-6E, 1998.
- [4] N. Duraiswamy, R. T. Schoepfhoerster, M. R. Moreno, and J. E. Moore, "Stented artery flow patterns and their effects on the artery wall," *Ann Rev Fluid Mech*, vol.39, pp. 357-382, 2007.
- [5] C. Rogers and E. R. Edelman, "Endovascular stent design dictates experimental restenosis and thrombosis," *Circulation*, vol. 91, pp. 2995-3001, 1995.
- [6] F. Auricchio, M. Di Loreto, and E. Sacco, "Finite-element analysis of a stenotic artery revascularization through a stent insertion," *Comput Methods Biomech Biomed Engin*, vol. 4, pp. 249-263, 2001.
- [7] F. Migliavacca, L. Petrini, P. Massarotti, S. Schievano, F. Auricchio, and G. Dubini, "Stainless and shape memory alloy coronary stents: a computational study on the interaction with the vascular wall," *Biomech Model Mechanobiol* vol. 2, pp. 205-217, 2004.
- [8] C. Lally, F. Dolan, and P. J. Prendergast, "Cardiovascular stent design and vessel stresses: a finite element analysis," *J Biomech*, vol. 38, pp. 1574-1581, 2005.
- [9] D. K. Liang, D. Z. Yang, M. Qi, and W. Q. Wang, "Finite element analysis of the implantation of a balloon-expandable stent in a stenosed artery," *Int J Cardiol*, vol. 104, pp. 314-318, 2005.
- [10] J. Bedoya, C. A. Meyer, L. H. Timmins, M. R. Moreno, and J. E. Moore, "Effects of stent design parameters on normal artery wall mechanics," *J Biomech Eng*, vol. 128, pp. 757-765, 2006.
- [11] G. Holzapfel, M. Stadler, and C. Schulze-Bauer, "A layer-specific three-dimensional model for the simulation of balloon angioplasty using magnetic resonance imaging and mechanical testing," *Ann Biomed Eng*, vol. 30, pp. 753-767, 2002.
- [12] D. Kioussis, T. Gasser, and G. Holzapfel, "A numerical model to study the interaction of vascular stents with human atherosclerotic lesions," *Ann Biomed Eng*, vol. 35, pp. 1857-1869, 2007.
- [13] F. Gijssen, F. Migliavacca, and S. Schievano, "Simulation of stent deployment in a realistic human coronary artery," *BioMed Eng OnLine*. vol. 7, 2008.
- [14] C. K. Chang, C. P. Huded, B. W. Nolan, and R. J. Powell, "Prevalence and clinical significance of stent fracture and deformation following carotid artery stenting," *J Vasc Surg*. vol. 54, pp. 6856-6890, 2001.
- [15] T. Tsunoda, H. Hara, K. Nakajima, H. Shinji, et al., "Stent deformation: an experimental study of coronary ostial stenting," *Cardiovasc Revasc Med*, vol. 10, pp. 80-87, 2009.
- [16] E. Babalik, M. Gulbaran, T. Gurmen, and S. Ozturk, "Fracture of popliteal artery stents," *Circ J*. vol.67, pp. 643-645, 2003.
- [17] J. Solis, S. Allaqaband, and T. Bajwa, "A case of popliteal stent fracture with pseudoaneurysm formation," *Catheter Cardiovasc Interv*. vol. 67, pp. 319-322, 2006.
- [18] D. Scheinert, S. Scheinert, J. Sax, et al., "Prevalence and clinical impact of stent fractures after femoropopliteal stenting," *J Am Coll Cardiol*. vol. 45, pp. 312-315, 2005.
- [19] S. A. Berger, W. Goldsmith, and E. R. Lewis, Eds., "Introduction to Bioengineering," New York, NY: Oxford University Press, 1996.
- [20] B. M. Johnston, P. R. Johnston, S. Corney, and D. Kilpatrick, "Non-Newtonian blood flow in human right coronary arteries: steady state simulations," *J Biomech.*; vol. 37, no. 5, pp. 709-720, May 2004.
- [21] J. A. Moore, D. A. Steinman, S. Prakash, K. W. Johnston, and C. R. Ethier, "A numerical study of blood flow patterns in anatomically realistic and simplified end-to-side anastomoses," *J. Biomech. Eng*, vol. 121, pp. 265-272, 1999.



Hiroshi Okada was born in Kagoshima, Japan. He received B.S. degree in mechanical engineering from Tokyo University of Science, Chiba, Japan, in 1986, and Ph.D. degree in computational mechanics in School of Civil Engineering at Georgia Institute of Technology, Atlanta, USA in 1990.

He continued his postdoctoral training in Georgia Institute of Technology, Atlanta, USA until 1991. He then joined Nissan Research Center, Japan, as a RESEARCHER. From 1993 to 1996, he was appointed as a RESEARCH ENGINEER in Computational Mechanics Center, Georgia Institute of Technology, Atlanta, USA, and an ASSOCIATE PROFESSOR at Kagoshima University, Japan. Currently, he is a PROFESSOR in Department of Mechanical Engineering, Faculty of Science and Technology at Tokyo University of Science, Chiba, Japan. He is specialized in computational mechanics, Finite Element Method, Fracture Mechanics, and Simulation. Prof. Okada has served, and is serving, as a member of numerous technical committees of professional organizations such as Japan Society of Mechanical Engineers (JSME), Japan Society for Computational Engineering and Science (JSCES), Japan Association for Computational Mechanics (JACM), Japan Welding Engineering Society (JWES), and as editor for Journal of Computational Science and Technology, and as a scientific committee chair or as chair of programs, for conference of JSME, JSCES. He was awarded The K. Washizu Medal in 2008, Computational Mechanics Achievement Award from JSME and JACM Fellows Award in 2009.



Feng Gao was born in Shandong, China in 1977. He received B.S. degree in mechanical engineering from Nanjing Forest University, Jiangsu, China, in 2000, M.S. degree in mechanics from Beijing University of Technology, Beijing, China in 2003, and Ph.D. degree in information science in Japan Advanced Institute of Science and Technology, Ishikawa, Japan, in 2006.

He continued his postdoctoral training in Aalborg Hospital Science & Innovation Center, Aalborg, Denmark until 2008. He was a RESEARCH SCIENTIST in Department of Bioengineering at University of Washington, Seattle, USA, from 2008 to 2010. Currently, he is an ASSISTANT PROFESSOR in Department of Mechanical Engineering at Tokyo University of Science, Chiba, Japan. His research interests include biomechanics, computational modeling and numerical simulation in physiology, and fluid-structure interaction.

Dr. Gao is a member of Japan Society for Computational Engineering and Science.



Gang Li was born in Liaoning, China in 1977. He received M.D. degree from Hebei Medical University, Hebei, China, in 2001, and Ph.D. degree from Shinshu University Graduate School of Medicine, Matsumoto, Japan, in 2007.

He continued his postdoctoral training in Department of Metabolic Regulation, Shinshu University, Matsumoto, Japan until 2008.

Currently, he is an ASSOCIATE PROFESSOR in Cardiovascular Center of Hebei General hospital, Hebei, China. His research interests and clinical activities mainly dealt with prevention of complications after cardiac interventional therapy.